Beyond the Global Brain Differences: Intra-individual Variability Differences in 1q21.1 Distal and 15q11.2 BP1-BP2 Deletion Carriers

Rune Boen[1,2*], Tobias Kaufmann[2,3], Dennis van der Meer[2,4], Oleksandr Frei[2,5], Ingrid Agartz[6,7,8], David Ames[9,10], Micael Andersson[11,12], Nicola J. Armstrong[13], Eric Artiges[14,15], Joshua R. Atkins[16,17,18], Jochen Bauer[19], Francesco Benedetti[20,21], Dorret I.Boomsma[22], Henry Brodaty[23], Katharina Brosch[24], Randy L. Buckner[25,26], Murray J. Cairns[16,27], Vince Calhoun[28], Svenja Caspers[29,30], Sven Cichon[29,31,32], Aiden P.Corvin[33], Benedicto Crespo Facorro[34,35,36], Udo Dannlowski[37], Friederike S. David[38], Eco J.C. de Geus[22] ,

Greig I. de Zubicaray[39], Sylvane Desrivières[40], Joanne L. Doherty[41,42], Gary Donohoe[43], Stefan Ehrlich[44], Else Eising[45], Thomas Espeseth[46,47], Simon E. Fisher[45,48], Andreas J. Forstner[38,29], Lidia Fortaner Uyà[20,21], Vincent Frouin[49], Masaki Fukunaga[50], Tian Ge[51,52], David C. Glahn[53,54], Janik Goltermann[37], Hans J. Grabe[55], Melissa J. Green[56,57], Nynke A. Groenewold[58], Dominik Grotegerd[37], Tim Hahn[37], Ryota Hashimoto[59], Jayne Y. Hehir-Kwa[60], Frans A. Henskens[61,62], Avram J. Holmes[63,64], Asta K. Håberg[65,66] , Jan Haavik[67,68], Sebastien Jacquemont[69,70], Andreas Jansen[71,72], Christiane Jockwitz[29,30], Erik G. Jönsson[6,73], Masataka Kikuchi[74,75], Tilo Kircher[24], Kuldeep Kumar[76], Stephanie Le Hellard[77,78], Costin Leu[79,80], David E. Linden[81,82], Jingyu Liu[83,84], Robert Loughnan[85,86], Karen A. Mather[23], Katie L. McMahon[87], Allan F. McRae[88], Sarah E. Medland[89,90,91], Susanne Meinert[37], Clara A. Moreau[92], Derek W. Morris[93], Bryan J. Mowry[94,95], Thomas W. Mühleisen[29,30,96], Igor Nenadić[24], Markus M. Nöthen[38], Lars Nyberg[97], Michael J. Owen[41,98], Marco Paolini[20,21], Tomas Paus[99,100], Zdenka Pausova[101,102], Karin Persson[103,104], Yann Quidé[105,106], Tiago Reis Marques[107], Perminder S. Sachdev[23,108], Sigrid B.Sando[65,109], Ulrich Schall[110], Rodney J.Scott[111,112,113], Geir Selbæk[114,115,104,] Elena Shumskaya[48,116], Ana I.Silva[81], Sanjay M. Sisodiya[79,117], Frederike Stein[24], Dan J. Stein[118], Benjamin Straube[24], Fabian Streit[119,], Lachlan T. Strike[89,120], Alexander Teumer[121,55,122], Lea Teutenberg[24], Anbupalam Thalamuthu[23], Paul A Tooney[16,123], Diana Tordesillas-Gutierrez[124,25], Julian N Trollor[126,127] Dennis van 't Ent[128], Marianne B.M. van den Bree[129,130], Neeltje E.M. van Haren[131,132], Javier Vázquez-Bourgon[133,134,35], Henry Völzke[135,122], Wei Wen[23], Katharina Wittfeld[55], Christopher R.K. Ching[92], Lars T. Westlye[2,46,136], Paul M. Thompson[92], Carrie E. Bearden[137], Kaja K. Selmer[138], Dag Alnæs[2,139], Ole A. Andreassen[2,6,136], Ida E. Sønderby[1,2,136]

1 Department of Medical Genetics, Oslo University Hospital, Oslo, Norway

2 NORMENT, Division of Mental Health and Addiction, Oslo University Hospital and Institute of Clinical Medicine, University of Oslo, Oslo, Norway

3 Department of Psychiatry and Psychotherapy, Tübingen Center for Mental Health, University of Tübingen, Germany

4 School of Mental Health and Neuroscience, Faculty of Health, Medicine and Life Sciences, Maastricht University, Maastricht, Netherlands

5 Centre for Bioinformatics, Department of Informatics, University of Oslo, Oslo, Norway

6 NORMENT, Institute of Clinical Medicine, University of Oslo, Oslo, Norway

7 Department of Clinical Research, Diakonhjemmet Hospital, Oslo, Norway

8 Centre for Psychiatry Research, Department of Clinical Neuroscience, Karolinska Institutet & Stockholm Health Care Services, Stockholm, Sweden

9 University of Melbourne Academic Unit for Psychiatry of Old Age, St George's Hospital, Kew, VIC, Australia

10 National Ageing Research Institute, Parkville, VIC, Australia

11 Department of Integrative Medical Biology (IMB), Umeå University, Umeå, Sweden

12 Umeå Center for Functional Brain Imaging, Umeå University, Umeå, Sweden

13 Mathematics & Statistics, Curtin University, Perth, WA, Australia

14 INSERM U1299, ENS Paris Saclay, Université Paris Saclay, Gif-sur-Yvette, France

15 EPS Barthelemy Durand, Etampes, France

16 School of Biomedical Sciences and Pharmacy, University of Newcastle, Callaghan, NSW, Australia

17 Precision Medicine Research Program, Hunter Medical Research Institute, Newcastle, NSW, Australia

18 The Cancer Epidemiology Unit, Nuffield Department of Population Health, University of Oxford, Oxford, UK

19 University Clinic for Radiology, University of Münster, Muenster, Germany

20 University Vita-Salute San Raffaele, Milano, Italy

21 Psychiatry & Clinical Psychobiology, Division of Neuroscience, Scientific Institute Ospedale San Raffaele, Milano, Italy

22 Department of Biological Psychology, Vrije Universiteit Amsterdam, Amsterdam, NH, Netherlands

23 Centre for Healthy Brain Ageing, University of New South Wales, Sydney, NSW, Australia

24 Department of Psychiatry and Psychotherapy, Philipps-University Marburg, Marburg, Germany

25 Psychology and Center for Brain Science. Harvard University, Cambridge, MA, USA

26 Psychiatry, Massachusetts General Hospital, Boston, MA, USA

27 Precision Medicine Research Program, Hunter Medical Research Institute, New Lambton Heights, NSW, Australia

28 Tri-institutional Center for Translational Research in Neuroimaging and Data Science (TReNDS), Georgia State, Georgia Tech, Emory, Atlanta, GA 30303, USA

29 Institute of Neuroscience and Medicine (INM-1), Research Centre Jülich, Jülich, Germany

30 Institute for Anatomy I, Medical Faculty & University Hospital Düsseldorf, Heinrich Heine University Düsseldorf, Düsseldorf, Germany

31 University of Basel, Basel, Switzerland

32 University Hospital Basel, Basel, Switzerland

33 Department of Psychiatry, Trinity College Dublin, Dublin, Ireland

34 Hospital Universitario Virgen del Rocío/ IBIS/ CSICC, Sevilla, Spain

35 Centro de Investigación Biomedica en Red Salud Mental (CIBERSAM), Sevilla, Spain

36 Department of Psychiatry, University of Sevilla, Sevilla, Spain

37 Institute for Translational Psychiatry, University of Münster, Münster, Germany

38 Institute of Human Genetics, University of Bonn, School of Medicine & University Hospital Bonn, Bonn, Germany

39 School of Psychology and Counselling, Queensland University of Technology, Brisbane, QLD, Australia

40 Social Genetic and Developmental Psychiatry Centre, Institute of Psychiatry, Psychology & Neuroscience, King's College London, London, UK

41 Centre for Neuropsychiatric Genetics and Genomics, Cardiff University, Cardiff, UK

42 Cardiff University's Brain Research Imaging Centre, School of Psychology, Cardiff University, Cardiff, UK

43 School of Psychology & Center for Neuroimaging, Cognition and Genomics, University of Galway, Galway, Ireland

44 Translational Developmental Neuroscience Section, Division of Psychological and Social Medicine and Developmental Neurosciences, Faculty of Medicine, TU Dresden, Germany

45 Language and Genetics Department, Max Planck Institute for Psycholinguistics, Nijmegen, Netherlands

46 Department of Psychology, University of Oslo, Oslo, Norway

47 Department of Psychology, Oslo New University College, Oslo, Norway

48 Donders Institute for Brain, Cognition and Behaviour, Radboud University, Nijmegen, Netherlands

49 Université Paris-Saclay, Neurospin, CEA, Gif sur Yvette, France

50 Division of Cerebral Integration, National Institute for Physiological Sciences, Okazaki, Japan

51 Psychiatric and Neurodevelopmental Genetics Unit, Center for Genomic Medicine, Massachusetts General Hospital, Boston, MA, USA

52 Department of Psychiatry, Massachusetts General Hospital, Harvard Medical School, Boston, MA, USA

53 Department of Psychiatry and Behavioral Sciences, Boston Children's Hospital, Boston, MA, USA

54 Department of Psychiatry, Harvard Medical School, Boston, MA, USA

55 Department of Psychiatry and Psychotherapy, University Medicine Greifswald, Greifswald, Germany

56 Discipline of Psychiatry and Mental Health, School of Clinical Medicine, University of New South Wales, Sydney, NSW, Australia

57 Neuroscience Research Australia, Sydney, NSW, Australia

58 Department of Psychiatry & Mental Health, Neuroscience Institute, University of Cape Town, Cape Town, South Africa

59 Department of Pathology of Mental Diseases, National Institute of Mental Health, National Center of Neurology and Psychiatry, Kodaira, Tokyo, Japan

60 Princess Máxima Center for Pediatric Oncology, Utrecht, Netherlands

61 School of Medicine and Public Health, University of Newcastle, Newcastle, NSW, Australia

62 PRC for Health Behaviour, University of Newcastle, Newcastle, NSW, Australia

63 Psychiatry, Rutgers University, New Brunswick, NJ, USA

64 Brain Health Institute, Rutgers University, Piscataway, NJ, USA

65 Department of Neuromedicine and Movement Science (INB), Faculty of Medicine and Health Sciences, NTNU, Trondheim, Norway

66 Department of Radiology and Nuclear Medicine, St. Olav's Hospital, Trondheim, Norway

67 Department of Biomedicine, University of Bergen, Bergen, Norway

68 Division of Psychiatry, Haukeland University Hospital, Bergen, Norway

69 Sainte Justine Hospital Research Center, Montreal, QC, Canada

70 Department of Pediatrics, University of Montreal, QC, Canada

71 Core-Facility Brainimaging, Marburg, Germany

72 Department of Psychiatry, Marburg, Germany

73 Centre for Psychiatry Research, Department of Clinical Neuroscience, Karolinska Institutet & Stockholm Health Care Services, Stockholm Region, Stockholm, Sweden

74 Department of Genome Informatics, Graduate School of Medicine, Osaka University, Osaka, Japan

75 Department of Computational Biology and Medical Sciences, Graduate School of Frontier Science, The University of Tokyo, Chiba, Japan

76 Centre de recherche CHU Sainte-Justine and University of Montréal, Montral, QC, Canada

77 NORMENT, Department of Clinical Science, University of Bergen, Bergen, Norway

78 Dr. Einar Martens Research Group for Biological Psychiatry, Center for Medical Genetics and Molecular Medicine, Haukeland University Hospital, Bergen, Norway

79 Department of Clinical and Experimental Epilepsy, Institute of Neurology, University College London, London, UK

80 Genomic Medicine Institute, Lerner Research Institute, Cleveland Clinic, Cleveland, OH, USA

81 Neuroscience and Mental Health Innovation Institute, Cardiff University, Cardiff, UK

82 School for Mental Health and Neuroscience, Department of Psychiatry and Neuropsychology, Faculty of Health, Medicine and Life Sciences, Maastricht University, Maastricht, Netherlands

83 Department of Computer Science, Georgia State University, GA, USA

84 Center for Translational Research in Neuroimaging and Data Science, Georgia State University, Atlanta, GA, USA

85 Department of Cognitive Science, University of California San Diego, La Jolla, CA, USA

86 Population Neuroscience and Genetics, University of California San Diego, La Jolla, CA, USA

87 School of Clinical Sciences, Queensland University of Technology, Brisbane, QLD, Australia

88 Institute for Molecular Bioscience, The University of Queensland, Brisbane, Australia

89 Psychiatric Genetics, QIMR Berghofer Medical Research Institute, Brisbane, QLD, Australia

90 University of Queensland, Brisbane, QLD, Australia

91 Queensland University of Technology, Brisbane, QLD, Australia

92 Imaging Genetics Center, Mark and Mary Stevens Institute for Neuroimaging and Informatics, Keck School of Medicine, University of Southern California, Marina del Rey, CA, USA.

93 Centre for Neuroimaging, Cognition and Genomics, School of Biological and Chemical Sciences, University of Galway, Galway, Ireland

94 Queensland Brain Institute, The University of Queensland, Brisbane, QLD, Australia

95 Queensland Centre for Mental Health Research, The University of Queensland, QLD, Australia

96 Department of Biomedicine, University of Basel, Basel, Switzerland

97 Department of Radiation Sciences and Integrative Medical Biology, Umeå University, Umeå, Sweden

98 Division of Psychological Medicine and Clinical Neurosciences, Cardiff University, Cardiff, UK

99 Departments of Psychiatry and Neuroscience, Faculty of Medicine and Centre Hospitalier Universitaire Sainte-Justine, University of Montreal, Montreal, QC, Canada

100 Departments of Psychiatry and Psychology, University of Toronto, ONT, Canada

101 The Hospital for Sick Children, Toronto, ON, Canada

102 Department of Physiology, University of Toronto, Toronto, ON, Canada

103 The Norwegian National Centre for Ageing and Health, Dept. of Geriatric Medicine, Vestfold Hospital Trust, Tønsberg, Norway

104 Department of Geriatric Medicine, Oslo University Hospital, Oslo, Norway

105 School of Psychology, The University of New south Wales, Sydney, NSW, Australia

106 Neuroscience Research Australia, Randwick, NSW, Australia

107 Psychosis Studies, Institute of Psychiatry, Psychology and Neuroscience, King's College London, London, UK

108 Neuropsychiatric Insitute, The Prince of Wales Hospital,Sydney, NSW, Australia

109 Department of Neurology and Clinical Neurophysiology, University Hospital of Trondheim, Trondheim, Norway

110 Hunter Medical Research Institute, Newqcastle, NSW, Australia

111 School of Biomedical Sciences and Pharmacy, College of Medicine, Health and Wellbeing, University of Newcastle, Newcastle, NSW, Australia

112 Division of Molecular Medicine, NSW Health Pathology, Newcastle, NSW, Australia

113 Level 3 West, Hunter Medical Research Institute, Newcastle, NSW, Australia

114 Norwegian Centre for Ageing and Health, Vestfold Hospital Trust, Tønsberg, Norway

115 Faculty of Medicine, University of Oslo, Oslo, Norway

116 Department of Human Genetics, Radboud University Medical Center, Nijmegen, Netherlands

117 Chalfont Centre for Epilepsy, Chalfont St Peter, UK

118 SAMRC Unit on Risk & Resilience in Mental Disorders, Dept of Psychiatry & Neuroscience Institute, University of Cape Town, Cape Town, South Africa

119 Department of Genetic Epidemiology in Psychiatry, Central Institute of Mental Health, Medical Faculty Mannheim, University of Heidelberg, Mannheim, Germany

120 School of Psychology and Counselling, Faculty of Health, Queensland University of Technology, Brisbane, Australia

121 Institute for Community Medicine, University Medicine Greifswald, Greifswald, Germany

122 German Centre for Cardiovascular Research (DZHK), Greifswald, Germany

123 Hunter Medical Research Institute, New Lambtion Heights, NSW, Australia

124 Instituto de Física de Cantabria UC-CSIC, Santander, Spain

125 Department of Radiology, Marqués de Valdecilla University Hospital, Valdecilla Biomedical Research Institute IDIVAL, Santander, Spain

126 Department of Developmental Disability Neuropsychiatry, University of New South Wales, Sydney, NSW, Australia

127 Centre for Healthy Brain Ageing, University of New South Newcastle, NSW, Australia

128 Biological Psychology & Netherlands Twin Register, Vrije Universiteit Amsterdam, NH, Netherlands

129 Institute of Psychological Medicine and Clinical Neurosciences, Cardiff, UK

130 Centre for Neuropsychiatric Genetics and Genomics, Cardiff, UK

131 Erasmus Medical Centre - Sophie, Rotterdam, Netherlands

132 University Medical Centre Utrecht, Utrecht, Netherlands

133 Department of Psychiatry, University Hospital Maqués de Valdecilla - IDIVAL, Santander, Spain

134 Departamento de Medicina y Psiquiatría, Universidad de Cantabria, Santander, Spain

135 University Medicine Greifswald, Institute for Community Medicine, Greifswald, Germany

136 KG Jebsen Centre for Neurodevelopmental Disorders, University of Oslo, Oslo, Norway.

137 Semel Institute for Neuroscience and Human Behavior, Departments of Psychiatry and Biobehavioral Sciences and Psychology, University of California Los Angeles, Los Angeles, CA, USA.

138 Department of Research and Innovation, Division of Clinical Neuroscience, Oslo University Hospital and the University of Oslo, Norway.

139 Kristiania University College, Oslo, Norway

*Correspondence:

Postal address: Department of Medical Genetics, Oslo University Hospital, Postbox 4956, Nydalen, 0424 Oslo, Norway

E-mail: boenrune@gmail.com

Keywords: copy number variants, 1q21.1 distal, 15q11.2 BP1-BP2, intra-individual variability, magnetic resonance imaging, brain structure

Abstract

Background: The 1q21.1 distal and 15q11.2 BP1-BP2 CNVs exhibit regional and global brain differences compared to non-carriers. However, interpreting regional differences is challenging if a global difference drives the regional brain differences. Intra-individual variability measures can be used to test for regional differences beyond global differences in brain structure.

Methods: Magnetic resonance imaging data were used to obtain regional brain values for 1q21.1 distal deletion (n=30) and duplication (n=27), and 15q11.2 BP1-BP2 deletion (n=170) and duplication (n=243) carriers and matched non-carriers (n=2,350). Regional intra-deviation (RID) scores i.e., the standardized difference between an individual's regional difference and global difference, were used to test for regional differences that diverge from the global difference.

Results: For the 1q21.1 distal deletion carriers, cortical surface area for regions in the medial visual cortex, posterior cingulate and temporal pole differed less, and regions in the prefrontal and superior temporal cortex differed more than the global difference in cortical surface area. For the 15q11.2 BP1-BP2 deletion carriers, cortical thickness in regions in the medial visual cortex, auditory cortex and temporal pole differed less, and the prefrontal and somatosensory cortex differed more than the global difference in cortical thickness.

Conclusion: We find evidence for regional effects beyond differences in global brain measures in 1q21.1 distal and 15q11.2 BP1-BP2 CNVs. The results provide new insight into brain profiling of the 1q21.1 distal and 15q11.2 BP1-BP2 CNVs, with the potential to increase our understanding of mechanisms involved in altered neurodevelopment.

Introduction

Carriers of certain rare recurrent copy number variants (CNVs) - i.e., deletions or duplications of a segment of the genome - have a higher risk of developing psychiatric and neurodevelopmental disorders, including schizophrenia and autism spectrum disorder[1–5] Several rare recurrent CNVs have moderate to large effects on structural brain measures derived from magnetic resonance imaging (MRI)[6,7]. The effects of CNVs on brain structure have been suggested to occur primarily during early neurodevelopment[8], and some rare recurrent CNVs have been associated with altered cellular function, composition and size derived from cortical organoids that models fetal and early neurodevelopment[9–12]. The 1q21.1 distal and 15q11.2 BP1-BP2 deletions are two of the most common recurrent CNVs[1,13,14]. They yield a higher risk of psychiatric and neurodevelopmental disorders[1–5] and show moderate to large effects on brain structure[15,16]. Thus, studying 1q21.1 distal and 15q11.2 BP1-BP2 deletion carriers offer a promising genetics-first approach to study deviations in neurodevelopment and brain structure, which may underlie the increased risk of developing psychiatric and neurodevelopmental disorders[5,8].

To date, the neuroimaging studies on CNVs have focused on conventional mean comparisons between carriers and non-carriers, which have been informative for brain profiling of CNV carriers. For instance, several CNVs have shown global effects on the brain, as demonstrated by group differences in mean cortical thickness, total cortical surface area and total subcortical volume, in addition to wide-spread regional differences[6,7]. However, brain profiling may be challenging if an overall global difference on the brain drives many of the regional mean differences or if regional differences are driven by distinct subgroups in each comparison, rendering inter-regional brain profiles difficult to interpret. To overcome this challenge, detecting brain regions that diverge from the global difference could benefit from intraindividual variability measures, in which regional values represent its position within an individualized brain profile. Identification of brain regions that diverge from the overall global difference of the CNV may provide valuable insights into the regional penetrance, brain organization and functional consequences in CNV carriers. Indeed, as has been demonstrated in other fields such as cognitive science and neuropsychology, e.g.[17–22], novel scientific and clinical insights can be achieved by looking beyond mean group differences through investigating intraindividual variability.

Both 1q21.1 distal and 15q11.2 BP1-BP2 deletion carriers exhibit global differences in brain structure, with the former displaying a lower total cortical surface area[15] and the latter showing a higher mean cortical thickness and lower total cortical surface area[16]. Additionally, these deletions also exhibit regional differences across the cortex[15,16]. However, the regional differences vary across the brain as indicated by variation in effect sizes across brain regions. This could indicate that the carriers of the 1q21.1 distal and 15q11.2 BP1-BP2 deletion exhibit higher variability in brain structure, along with systematic inter-regional differences in brain structure as measured by MRI-derived features.

In both 1q21.1 distal and 15q11.2 BP1-BP2 CNV carriers, the largest regional differences are typically found in frontal regions, associated with higher-cognitive processing. In contrast, the posterior brain regions, associated with primary sensory processing, typically do not show significant differences[15,16]. Insight into variation in brain structure may be useful for understanding differences in brain function as cortical morphology overlaps with the functional hierarchical gradient of the brain[23]. This functional hierarchical gradient reflects a sensorimotor (i.e., involved in unimodal and functional specific processes) to association axis (i.e., involved in higher-order cognitive processes) in the human brain[23–25], which has been supported by anatomical, functional, and evolutionary data[24]. Thus, a more fine-grained brain profile of the structural differences in 1q21.1 distal and 15q11.2 BP1-BP2 CNV carriers may aid our understanding of their phenotypic profile.

Brain structural differences in 1q21.1 distal and 15q11.2 BP1-BP2 CNV carriers indicate global mean differences (i.e., cortical thickness and cortical surface area), as well as regional group differences in primarily frontal brain regions. The regional group differences indicate that some brain regions are more affected than others. Here, we define more affected brain regions as regions that differ more than the global mean difference, and less affected brain regions as regions that differ less than the global mean difference. To measure this, we use an intraindividual variability measure to detect brain regions that diverge from the global difference, where the regional values represent its position within an individualized brain profile. We expected that anterior regions within the association cortices were more affected, whereas posterior regions within the primary sensorimotor cortices were less affected in carriers of the 1q21.1 distal and 15q11.2 BP1-BP2 CNVs.

Methods and Materials

Sample

Individuals carrying a 1q21.1 distal or 15q11.2 CNV and a matched non-carrier group were taken from the ENIGMA-CNV working group core dataset and the UK Biobank across 61 scanner sites. Each CNV carrier was matched with five non-carriers based on age, sex, scanner site and ICV using the MatchIt package in R[26]. This resulted in four subsets (sample characteristics are presented in tables 1 and 2, supplementary note 1).

[INSERT TABLE 1 HERE]

[INSERT TABLE 2 HERE]

MRI-derived features, CNVs and quality control

Neuroimaging data were obtained from the UK Biobank, as described elsewhere[27], and from the ENIGMA-CNV core dataset. The ENIGMA-CNV neuroimaging measures were collected from several sites (see appendix 1 for details) and analyzed using the standardized ENIGMA protocol (https://enigma.ini.usc.edu/protocols/imaging-protocols/). Details of the quality control of the MR images are provided in supplementary note 2. Briefly, the MRI data from the ENIGMA-CNV working group underwent the ENIGMA cortical quality control procedures (https://enigma.ini.usc.edu/protocols/imaging-protocols/), where the 68 cortical and 14 subcortical regions were extracted using the Desikan-Killiany atlas. For the UK Biobank sample, we used the Euler number as a proxy for image quality[28] and removed all participants with Euler numbers below minus four standard deviations from downstream analyses (n =437). To account for site effects in the samples, we ran each of the four subsets through ComBat, an instrument for data harmonization[29]. CNV calling in ENIGMA-CNV was based on previous publications[15,16]. For the UK Biobank sample, we identified CNVs based on the returned dataset from Crawford et al.[30] All participants with a CNV as defined in previous publications[15,16,30] were removed from downstream analyses, except for the individuals flagged with the 1q21.1 distal or the 15q11.2 BP1-BP2 CNV.

Derivation of dependent variables

We adjusted for the effect of age, age^2, sex and ICV on every brain regional value using linear regression across the carriers and the non-carriers. The residualized brain regional values were used to calculate the mean and standard deviation for the non-carriers only. We estimated 1) Z-scores per region (similar calculations as in[31]) and created 2) global index and 3) intraindividual standard deviation (similar calculations as in [21]) as well as 4) regional intra-deviation (RID) score.

1. Z-scores. Specifically, Z-scores for CNV carriers and non-carriers were calculated based on the mean and standard deviation from the non-carriers as shown in Eq. (1):

$$Z_{if} = \frac{(X_{if} - M_{if})}{SD_{if}}$$

(1)

Where Z_{if} is the standardized value for brain region *i* in feature *f* (i.e., cortical thickness, surface area, or subcortical volume), and X_{if} is the regional value for brain region *i* for feature *f*, M_{if} and SD_{if} represent the mean and standard deviation, respectively, for brain region *i* using feature *f* across the non-carriers. Thus, for every individual we obtained a vector of standardized Z-scores across 68 cortical regions for cortical thickness and cortical surface area, and 14 subcortical regions.

2. Global index: We created an individualized global index (GI) for cortical thickness, cortical surface area and subcortical volume, respectively, by calculating the mean Z-score across the cortical and subcortical regions as shown in Eq. (2)

$$GI_f = \frac{1}{n_f}\sum_{i=1}^{n_f} Z_{if}$$

(2)

where GI_f is the global index for feature *f*, n is the total number of brain regions for feature *f*, and Z_{if} is the standardized value for the brain region *I* for feature *f* derived from Eq. (1).

3. Intraindividual standard deviation: Furthermore, we also calculated the intraindividual standard deviation (iSD) across the Z-scores for cortical thickness, cortical surface area, and subcortical volume to obtain measures of within-individual variability, as shown in Eq. (3):

$$iSD_f = \sqrt{\frac{\sum_{i=1}^{n_f}\left(Z_{if} - GI_f\right)^2}{n_f - 1}}$$

(3)

where the n_f is total number of brain regions for feature *f*, Z_{if} is the standardized value for brain region *i* for feature *f*, GI_f is the global index for feature *f* (i.e., mean Z-score across brain regions for an individual) as derived from Eq. (2). A low iSD indicates that an individual's Z-scores across brain regions are relatively consistent and do not vary much across brain regions, while a high iSD indicates that the Z-score across brain regions are relatively inconsistent, indexing a more variable brain.

4. Regional intra-deviation score: Finally, to identify regions that diverge more than expected from an individual's global index and intraindividual standard deviation, we created a regional intra-deviation (RID) score calculated using Eq. (4) for every brain region across feature *f*:

$$RID_f = \frac{\left(Z_{if} - GI_f\right)}{iSD_f}$$

(4)

where the Z_{if} is the standardized value for brain region *i* for feature *f*, and GI_f is the global index for feature *f* as shown in Eq. (2.). The iSD_f reflects the standard deviation for the Z-score across brain regions in feature *f* as formulated in Eq. (3). Here, we define regions that are less affected as those that do not follow the global tendency in the data, whereas the regions that exceed the global tendency of the data are considered to be more affected. To establish brain-cognition relationships between the brain measures and cognition, we tested for associations between RID and Z-scores and cognitive ability (supplementary note 3, Figure S1, Table S1).

Statistical analyses

All statistical analyses were conducted in R studio v4.0.0 and brain visualizations were created using the ENIGMA toolbox[32]. For the per-CNV analyses, we tested for group differences by including carrier status (i.e., either carrier or non-carrier) in a linear regression model. The deletion and duplication carriers were tested separately with their corresponding matched non-carrier group used as the reference. The estimated standardized beta values were extracted from the models and are presented in the results as a measure of effect size. The p-values underwent a False Discovery Rate (FDR)[33] adjustment to account for multiple comparisons for each of the four CNV groups. Corrected p-values below .05 were considered statistically significant. Three main analyses were performed: First, in line with the conventional mass-univariate analysis approach, we performed group comparisons on the Z-scores across all the ROIs for cortical thickness, cortical surface area and subcortical volume (FDR corrected for 150 comparisons). Second, we compared the global index, and intraindividual standard deviation and mean corrected intraindividual standard deviation values between carriers and non-carriers (FDR corrected for 12 comparisons). The mean corrected intraindividual standard deviation represents the intraindividual standard deviation after regressing out the global index, as the mean values tend to be correlated with the standard deviation. Third, for the RID scores, group comparisons were computed between carriers and non-carriers for all ROIs for cortical thickness, cortical surface area, and subcortical volume (FDR corrected for 150 comparisons). Due to missing values in some brain regions, the analyses were restricted to individuals with complete observations for the feature that was analyzed (i.e., cortical thickness, cortical surface area, and subcortical volume). Sensitivity analyses were conducted for the significant RID score differences by adjusting for affection status (i.e., known psychiatric or neurological diagnoses). In addition, we examined the interaction term between carrier status and affection status and between carrier status and cognitive ability. Finally, we compared the brain profile of significant differences in RID scores to the significant differences in Z-scores adjusted for the global index.

Results

Global measures

The group differences in the global index and the intraindividual standard deviation measures are presented in Table 3 with reference values for the non-carrier groups in Table S2. The 1q21.1 distal deletion carriers had a lower global index for surface area, whereas the 15q11.2 BP1-BP2 deletion carriers had a lower global index for surface area and a higher global index for cortical thickness. In addition, the 15q11.2 BP1-BP2 duplication carriers had a lower global index for cortical thickness. Furthermore, there was a higher intraindividual standard deviation for cortical surface for both the 1q21.1 distal duplication carriers (both for the mean corrected and uncorrected measure) and the 15q11.2 BP1-BP2 deletion carriers (only for the mean corrected measure), as well as a higher intraindividual standard deviation for cortical thickness in the 15q11.2 BP1-BP2 deletion carriers (both for the mean corrected and uncorrected measure). With one exception, correlations between the intraindividual standard deviation measures across CNV groups did not show any significant differences (supplementary note 4, Figure S2).

[INSERT TABLE 3 HERE]

1q21.1 distal copy number variant

The 1q21.1. distal deletion carriers showed widespread lower cortical surface area with significant differences in 63 ROIs using Z-scores (Figure 1a-b, top; Table S3), and exhibited a higher RID score for cortical surface area in regions within the occipital, superior parietal, temporal pole and posterior cingulate cortex, as well as lower RID scores in regions within the superior temporal and frontal regions (Figure 1a-c, bottom, Table S4). Further, 1q21.1. distal deletion carriers showed higher cortical thickness compared to non-carriers in 19 ROIs using Z-scores (Figure 2a-b, top, Table S3), in addition to lower RID scores for regions within the occipital lobe and paracentral lobule and higher RID scores for regions within the superior temporal and inferior frontal cortex (Figure 2a-c, bottom, Table S4). The 1q21.1 distal deletion carriers also exhibited lower subcortical volume in left thalamus and right nucleus accumbens (Table S3), and lower RID score for the left thalamus (Table S4). All the significant RID score differences survived adjustment for affection status. The interaction term between carrier status and affection status was not associated with the significant RID scores (supplementary note 5, Table S5). A subset of the significant RID scores were implicated in the brain-cognition RID map (Figure S1). However, we did not observe any significant interactions between carrier status and cognitive ability on any of the significant RID scores (supplementary note 6, Table S6). The results yielded more significant group differences in RID scores (i.e., 24) compared to Z-scores adjusted for the global index between 15q11.2 BP1-BP2 deletion carriers and non-carriers (i.e., 13, supplementary note 7, Figure S3, Table S7). ***The 1q21.1 distal duplication*** carriers showed higher cortical surface area in the right pars opercularis and right superior frontal gyrus, and lower volume in the right and left hippocampus compared to non-carriers (Table S8). Using RID scores, no significant differences in the ROIs were found (Table S9).

[INSERT FIGURE 1 HERE]

[INSERT FIGURE 2 HERE]

15q11.2 BP1-BP2 copy number variant

The 15q11.2 BP1-BP2 deletion carriers showed lower cortical surface area in 10 ROIs using Z-scores (Figure 3a-b, top, Table S10), and higher RID scores for the left frontal pole and right pars opercularis surface area, but lower RID scores for the left and right pars orbitalis surface area compared to non-carriers (Figure 3a-c, bottom, Table S11). For cortical thickness, the 15q11.2 BP1-BP2 deletion carriers showed higher cortical thickness in 30 regions using Z-scores (Figure 4a-b, top, Table S10). The RID scores for cortical thickness were lower in regions within occipital and temporal regions, and higher in motor and frontal regions compared to non-carriers (Figure 4a-c, bottom, Table S11). The 15q11.2 BP1-BP2 deletion carriers also showed lower Z-scores for left caudate, right pallidum and right nucleus accumbens (Table S10). All significant RID scores remained significant after adjustment for affection status. No significant interactions between carrier status and affection status (Table S12, supplementary note 5) nor between carrier status and cognitive ability for the 15q11.2 BP1-BP2 deletion carriers were observed (Table S13, supplementary note 6). The results yielded more significant group differences in RID scores (i.e., 14) compared to Z-scores adjusted for global index (i.e., 12) between 15q11.2 BP1-BP2 deletion carriers and non-carriers (supplementary note 7, Figure S4, Table S14). ***The 15q11.2 BP1-BP2 duplication*** carriers showed lower cortical thickness in 11 ROIs and higher right superior frontal cortical surface area using Z-scores (Table S15) but showed no significant differences in the ROIs using RID-scores (Table S16).

[INSERT FIGURE 3 HERE]

[INSERT FIGURE 4 HERE]

Discussion

The current study is the first to identify intraindividual variability differences in brain structure in CNV carriers. Using the intraindividual standard deviation measure, we observed higher variability in the regional effects for cortical surface area in both 1q21.1 distal duplication and 15q11.2 BP1-BP2 deletion carriers, and higher variability in the regional effects for cortical thickness for the 15q11.2 BP1-BP2 deletion carriers, compared to non-carriers. Using RID scores, we find that a subset of brain regions diverged significantly from non-carriers for both the 1q21.1 distal and 15q11.2 BP1-BP2 deletion carriers. We also find a higher number of significant regional differences using RID scores compared to the conventional global covariation approach. The current results hold promise for identifying specific CNV-associated brain profiles by targeting regional differences using an individualized approach, which are overlooked in studies applying conventional brain MRI measures.

In line with previous results[15], the 1q21.1 distal deletion carriers showed lower global cortical surface area compared to non-carriers. The observed differences in Z-scores indicate widespread lower cortical surface area, whereas the RID scores indicate that the cortical surface area in posterior and primary sensory regions (i.e., lingual, pericalcarine, superior parietal, isthmus of the cingulate gyrus) are less affected and frontal and association cortices (i.e., caudal middle frontal, lateral orbitofrontal, rostral middle frontal, superior frontal cortex) are more affected. Thus, the observed regional Z-score group differences along lateral and medial parietal to lateral inferior temporal and motor cortex appear to be largely reflective of the global effect. A subset of the significant RID scores (i.e., the superior temporal gyri and left supramarginal gyrus cortical thickness and left lateral orbitofrontal and left lateral superior temporal gyrus cortical surface area) was associated with cognitive ability in non-carriers. However, the effect sizes are low, and the current sample size of CNV carriers is too small to reliably detect such brain-cognition associations.

The 15q11.2 BP1-BP2 deletion showed a higher global cortical thickness compared to non-carriers, primarily concentrated in the frontal cortex, recapitulating previously reported group differences in cortical thickness[16]. We complement these findings by showing group differences in RID scores, which indicates that the cortical thickness in sensory cortices (i.e., cuneus and pericalcarine area) are less affected, and the association cortices (i.e., rostral middle frontal and superior frontal cortex) are more affected by the deletion. The association cortices that show cortical thickness differences using RID scores are regions that underlies complex cognitive functions[23–25], and may subserve the lower cognitive performance in 15q11.2 BP1-BP2 deletion carriers compared to controls[14,34].

Notably, some findings deviate from the interpretation of a less affected sensorimotor cortex and a more affected association cortex. Both the 1q21.1 distal and 15q11.2 BP1-BP2 deletion carriers show evidence for a relatively less affected cortical surface area and cortical thickness, respectively, in the left temporal pole. We also find that the cortical thickness of the postcentral gyri, a primary somatosensory region, is more affected in the 15q11.2 BP1-BP2 deletion carriers. To speculate, this may be associated with the motor delay observed in clinically affected 15q11.2 BP1-BP2 deletion carriers[35]. For cortical surface area in the 15q11.2 BP1-BP2 deletion carriers, we find inconsistent effects for frontal regions: although we observe a relatively more different bilateral pars orbitalis, we also find evidence for a less different left frontal pole and right pars opercularis. Furthermore, we did not find significant differences in RID scores in the 15q11.2 BP1-BP2 duplication carriers, nor in the 1q21.1

distal duplication carriers. The results complement previous findings of lower effect sizes in brain measures for duplication versus deletion carriers[6,7], and thus may support that deletion carriers distort the anatomical relationships in the brain more than duplication carriers.

Global and frontal regional group differences in cortical thickness are prominent brain features of several neurodevelopmental disorders, including autism spectrum disorder[36] and schizophrenia[37]. Thus, group differences in brain structure may be confounded by individuals with neurodevelopmental or psychiatric disorders. Here, all the significant RID score differences in 1q21.1 distal and 15q11.2 BP1-BP2 deletions survived adjustment for affection status, and there were no interaction effects between carrier status and affection status on the significant RID scores.

The current results implicate novel mechanisms in neurodevelopment. Compelling candidates for the changes in the 1q21.1 distal CNV are the human specific *NOTCH2NL* genes, which have been linked to the evolutionary expansion of the human neocortex[38,39]. NOTCH signaling is important for outer radial glia cell self-renewal, which are thought to contribute to cortical expansion[40]. Deletion of the *NOTCH2NL* genes in human cortical organoids yields smaller organoids compared to controls[38] and *NOTCH2NL* increases the number of cycling basal progenitors in the mouse embryonic neocortex[41]. Thus, *NOTCH2NL* could yield a potential mechanistic link between the assumed lower gene expression levels in 1q21.1 distal deletion carriers and the lower cortical surface area, possibly important for the expansion of frontal regions.

Among the four genes in the 15q11.2 BP1-BP2 loci[42], *CYFIP1* has gained considerable interest due to its association to schizophrenia[43,44] and autism[45–47]. *CYFIP1* exhibits high expression levels in the developing mouse brain[47]. *CYFIP1* has also been linked to variation in cortical surface area[48], as well as various cellular phenotypes, including myelination[49], neurite length and branch number, cell size[50], dendritic spine formation[51] and regulation of radial glia cells[52]. Notably, *CYFIP1* haploinsufficiency lower myelination thickness in rats[49]. Cortical thickness, as estimated with MRI, has been suggested to be influenced by myelination[53]. Thus, the higher cortical thickness observed in 15q11.2 BP1-BP2 deletion carriers may be due to altered myelination in the brain, possibly with somatosensory cortex being particularly sensitive to these alterations. *CYFIP1* deficiency has also been associated with functional connectivity deficits in motor cortices, as well as aberrant motor coordination in mice[54]. Finally, it should be noted that the 1q21.1 distal and the 15q11.2 BP1-BP2 loci span several genes, and genes within CNVs are likely to be involved in multifaceted genetic interactions[55]. More research is needed to identify the causative biological mechanisms of the brain structural phenotypes.

This study has strengths and limitations. We use an intraindividual variability approach to examine brain metrics that are related to an individual's own inter-regional brain profile. By examining metrics that consider the variation within individuals, it is possible to map the heterogeneity and deviations in CNV carriers compared to non-carriers. However, variability measures should be interpreted with caution, as some effects on the brain may be so extreme that further deviations are unlikely to be observed. That is, CNVs may yield large effects on brain structure, but only to a certain extent due to biological constraints. Thus, we urge caution when interpreting intraindividual standard deviation in brain measures as ceiling and floor effects may bias the variability metrics. Still, we identify structures that are significantly less different or more different relative to the mean difference, indicating sufficient variability in the individualized brain metrics. About 1/2 (1q21.1 distal) and 2/3 (15q11.2 BP1-BP2) of the carriers are derived from the UK Biobank, which has a healthy volunteer bias[56], possibly yielding underestimations of brain structural differences. However, this is somewhat counter-balanced by the ENIGMA-CNV dataset that is likely to increase the heterogeneity in the study sample (although some datasets are likely to have similar bias towards healthy individuals as the UK Biobank). Indeed, the variability observed in brain structure within individuals underscores the heterogeneity between and within individuals in the sample. Future studies with larger sample sizes are needed to examine the phenotypic heterogeneity observed in CNV carriers.

The results of the current study aid our understanding of 1q21.1 distal and 15q11.2 BP1-BP2 CNV brain profiles by identifying regional differences using intraindividual variability metrics, which has the potential to give better insight into the neuronal mechanisms in neurodevelopment and risk for psychiatric diseases. We find evidence for regional differences beyond the global differences in brain structure, where the spatial effects partly support the hypothesis of less affected sensorimotor cortex and more affected association cortex in both the 1q21.1 distal and 15q11.2 BP1-BP2 deletion carriers.

Acknowledgments

1000BRAINS: The 1000BRAINS-Study was funded by the Institute of Neuroscience and Medicine, Research Centre Jülich, Germany. We thank the Heinz Nixdorf Foundation (Germany) for the generous support of the Heinz Nixdorf Study. We also thank the scientists and the study staff of the Heinz Nixdorf Recall Study and 1000BRAINS. Furthermore, this project has received funding from the European Union's Horizon 2020 Research and Innovation Programme under Grant Agreement No. 945539 (HBP SGA3; SC). This research was additionally supported by the Joint Lab “Supercomputing and Modeling for the Human Brain”. We gratefully acknowledge the computing time granted through JARA-HPC on the supercomputer JURECA at Forschungszentrum Jülich.

TOP: Centre of Excellence: RCN #23273. RCN #. 226971.

ENIGMA-CNV working group: IES is supported by the Research Council of Norway (#223273), South-Eastern Norway Regional Health Authority (#2020060), European Union’s Horizon2020 Research and Innovation Programme (CoMorMent project; Grant #847776) and Kristian Gerhard Jebsen Stiftelsen (SKGJ-MED-021). RB is supported by South-Eastern Norway Regional Health Authority (#2020060). CEB is supported by NIMH U01MH119736, R21MH116473 and R01MH085953

This work was performed on Services for sensitive data (TSD), University of Oslo, Norway, with resources provided by UNINETT Sigma2 - the National Infrastructure for High Performance Computing and Data Storage in Norway.

ECHO-DEFINE: The ECHO study acknowledges funding from the Wellcome Trust (Institutional Strategic Support Fund (ISSF)) to Marianne B.M van den Bree and Clinical Research Training Fellowship to Joanne L. Doherty (102003/Z/13/Z)), the Waterloo

Foundation (WF 918- 1234 to Marianne B.M van den Bree), the Baily Thomas Charitable Fund (2315/1 to Marianne B.M van den Bree), National Institute of Mental Health (NIMH 5UO1MH101724 and NIMH U01MH119738 to Marianne B.M van den Bree), the IMAGINE-ID and IMAGINE-2 studies (funded by Medical Research Council (MRC; MR/N022572/1 and MR/T033045/1 to Marianne B.M van den Bree) and a Medical Research Council (MRC) Centre Grant to Michael J. Owen (MR/P005748/1). The DEFINE study was supported by a Wellcome Trust Strategic Award (100202/Z/12/Z) to Michael J. Owen.

UCLA-Utrecht: This study was supported by NIMH grant number: R01 MH090553 (to RAO). The NIMH had no further role in study design, in the collection, analysis and interpretation of the data, in the writing of the report, and in the decision to submit the paper for publication.

QTIM: The QTIM study was supported by grants from the US National Institute of Child Health and Human Development (R01 HD050735) and the Australian National Health and Medical Research Council (NHMRC) (486682, 1009064). Genotyping was supported by NHMRC (389875).

BETULA: Supported by a Scholar grant from Knut and Alice Wallenberg's (KAW) foundation to Lars Nyberg. Freesurfer calculations were enabled by resources provided by the Swedish National Infrastructure for Computing (SNIC) at HPC2N, Umeå.

SHIP: SHIP is part of the Community Medicine Research net of the University of Greifswald, Germany, which is funded by the Federal Ministry of Education and Research (grants no. 01ZZ9603, 01ZZ0103, and 01ZZ0403), the Ministry of Cultural Affairs and the Social Ministry of the Federal State of Mecklenburg-West Pomerania. Genome-wide data in SHIP have been supported by the Federal Ministry of Education and Research (grant no. 03ZIK012) and a joint grant from Siemens Healthcare, Erlangen, Germany and the Federal

State of Mecklenburg- West Pomerania. MRI scans in SHIP and SHIP-TREND have been supported by a joint grant from Siemens Healthcare, Erlangen, Germany and the Federal State of Mecklenburg-West Pomerania.

PAFIP: This work was supported by the Instituto de Salud Carlos III (00/3095, 01/3129, PI020499, PI14/00639, PI17/01056 and PI14/00918), SENY Fundació Research Grant CI2005 0308007 and Fundación Marqués de Valdecilla . Instituto de investigación sanitaria Valdecilla (A/02/07, NCT0235832 and NCT02534363).

OSAKA: This research was supported by AMED (grant number JP21wm0425012 and JP18dm0307002) and JSPS KAKENHI (grant number JP20H03611). This work was partially supported by JSPS KAKENHI (Grant Number JP22H04926 and 20K15778) and by grants from the Japan Agency for Medical Research and Development (AMED) (JP22wm0425012, JP22wm0525019, and JP22dk0207060). Some computations were performed at the Research Center for Computational Science, Okazaki, Japan (Project: NIPS, 18-IMS-C162, 19-IMS-C181, 20-IMS-C162, 21-IMS-C179, 22-IMS-C195).IMAGEN: received support from the European Union-funded FP6 Integrated Project IMAGEN (Reinforcement-related behavior in normal brain function and psychopathology) (LSHM-CT- 2007-037286), the Horizon 2020 funded ERC Advanced Grant 'STRATIFY' (Brain network based stratification of reinforcement-related disorders) (695313), the Medical Research Foundation and Medical Research Council (grants MR/R00465X/1 and MRF-058-0004-RG-DESRI: 'Neurobiological underpinning of eating disorders: integrative biopsychosocial longitudinal analyses in adolescents'; MR/S020306/1 and MRF-058-0009-RG-DESR-C0759: 'Establishing causal relationships between biopsychosocial predictors and correlates of eating disorders and their mediation by neural pathways'), the National Institutes of Health (NIH) funded Consortium grant U54 EB020403, supported by a cross-NIH alliance that funds Big Data to Knowledge Centres of Excellence, and 1R56AG058854-01, the National Institute for Health Research

(NIHR) Biomedical Research Centre (BRC) at South London and Maudsley NHS Foundation Trust (SLaM) and King's College London (KCL), ERANID (Understanding the Interplay between Cultural, Biological and Subjective Factors in Drug Use Pathways) (PR-ST-0416-10004), BRIDGET (JPND: BRain Imaging, cognition Dementia and next generation GEnomics) (MR/N027558/1), Human Brain Project (HBP SGA 2, 785907), the FP7 project MATRICS (603016), the Medical Research Council Grant 'c-VEDA' (Consortium on Vulnerability to Externalizing Disorders and Addictions) (MR/N000390/1), the Bundesministerium für Bildung und Forschung (BMBF grants 01GS08152; 01EV0711; Forschungsnetz AERIAL 01EE1406A, 01EE1406B), the Deutsche Forschungsgemeinschaft (DFG grants SM 80/7-2, SFB 940/2, NE 1383/14-1), the ANR (ANR-12-SAMA-0004, AAPG2019 – GeBra), the Eranet Neuron (AF12-NEUR0008-01 – WM2NA; and ANR-18-NEUR00002-01 – ADORe), the Fondation de France (00081242), the Fondation pour la Recherche Médicale (DPA20140629802), the Mission Interministérielle de Lutte-contre-les-Drogues-et-les-Conduites-Addictives (MILDECA), the Assistance-Publique-Hôpitaux-de-Paris and INSERM (interface grant), Paris Sud University IDEX 2012, the Fondation de l'Avenir (grant AP-RM-17-013), the Fédération pour la Recherche sur le Cerveau. Further support was provided by grants from: ANR (project AF12-NEUR0008-01 - WM2NA, and ANR-12-SAMA-0004), the Fondation de France, the Fondation pour la Recherche Médicale, the Mission Interministérielle de Lutte-contre-les-Drogues-et-les-Conduites-Addictives (MILDECA), the Assistance-Publique-Hôpitaux-de-Paris and INSERM (interface grant), Paris Sud University IDEX 2012; ANR (project AF12-NEUR0008-01 - WM2NA, ANR-12-SAMA-0004), the Eranet Neuron (ANR-18-NEUR00002-01), the Fondation de France (00081242), the Fondation pour la Recherche Médicale (DPA20140629802), the Mission Interministérielle de Lutte-contre-les-Drogues-et-les-Conduites-Addictives (MILDECA), the

Assistance-Publique-Hôpitaux-de-Paris and INSERM (interface grant), Paris Sud University IDEX 2012, the fondation de l'Avenir (grant AP-RM-17-013).

MCIC: The MCIC study was supported by the National Institutes of Health (NIH/NCRR P41RR14075 and R01EB005846 (to Vince D. Calhoun)), the Department of Energy (DE-FG02-99ER62764), the Mind Research Network, the Morphometry BIRN (1U24, RR021382A), the Function BIRN (U24RR021992-01, NIH.NCRR MO1 RR025758-01, NIMH 1RC1MH089257 to Vince D. Calhoun), the Deutsche Forschungsgemeinschaft (research fellowship to Stefan Ehrlich), and a NARSAD Young Investigator Award (to Stefan Ehrlich).

NTR: The NTR cohort was supported by the Netherlands Organization for Scientific Research (NWO) and The Netherlands Organisation for Health Research and Development (ZonMW) grants 904-61-090, 985-10-002, 912-10-020, 904-61-193, 480-04-004,463-06-001, 451-04-034, 400-05-717, Addiction-31160008, 016-115-035, 481-08-011, 056-32-010, Middelgroot-911-09-032, OCW_NWO Gravity programme—024.001.003, NWO-Groot 480-15-001/674, Center for Medical Systems Biology (CSMB, NWO Genomics), NBIC/BioAssist/RK(2008.024), Biobanking and Biomolecular Resources Research Infrastructure (BBMRI-NL, 184.021.007 and 184.033.111); Spinozapremie (NWO-56-464-14192), KNAW Academy Professor Award (PAH/6635) and University Research Fellow grant (URF) to Dorret I. Boomsma; Amsterdam Public Health research institute (former EMGO+), Neuroscience Amsterdam research institute (former NCA); the European Science Foundation (ESF, EU/QLRT-2001-01254), the European Community's Seventh Framework Programme (FP7- HEALTH-F4-2007-2013, grant 01413: ENGAGE and grant 602768: ACTION); the European Research Council (ERC Starting 284167, ERC Consolidator 771057, ERC Advanced 230374), Rutgers University Cell and DNA Repository (NIMH U24 MH068457-06), the National Institutes of Health (NIH, R01D0042157-01A1, R01MH58799-

03, MH081802, DA018673, R01 DK092127-04, Grand Opportunity grants 1RC2 MH089951 and 1RC2 MH089995); the Avera Institute for Human Genetics, Sioux Falls, South Dakota (USA). Part of the genotyping and analyses were funded by the Genetic Association Information Network (GAIN) of the Foundation for the National Institutes of Health. Computing was supported by NWO through grant 2018/EW/00408559, BiG Grid, the Dutch e-Science Grid and SURFSARA.

OATS: The OATS cohort has been funded by a National Health & Medical Research Council (NHMRC) and an Australian Research Council (ARC) Strategic Award Grant of the Ageing Well, Ageing Productively Program (ID No. 401162); NHMRC Project (seed) Grants (IDs 1024224, 1025243); NHMRC Project Grants (1045325, 1085606); and NHMRC Program Grants (568969, 1093083). OATS was facilitated through access to Twins Research Australia, a national resource supported by a Centre of Research Excellence Grant (1079102) from the National Health and Medical Research Council.

PING: The PING Project was supported by the National Institute on Drug Abuse and the Eunice Kennedy Shriver National Institute of Child Health and Human Development with the following awards: RC2DA029475 and R01 HD061414.

EPIGEN-UK (Sisodiya): The work was partly undertaken at UCLH/UCL, which received a proportion of funding from the UK Department of Health's NIHR Biomedical Research Centres funding scheme. We are grateful to the Wolfson Trust and the Epilepsy Society for supporting the Epilepsy Society MRI scanner.

Milan-OSR: The Milan-OSR cohort was supported by the European Union H2020 EU.3.1.1 grant 754740 MOODSTRATIFICATION, the Italian Ministry of Health, grant RF-2018-12367249 and the Italian Ministry of University and Scientific Research, grant A_201779W93T.

Dublin: The Dublin cohort was supported by grants to GD from the European Research Council (ERC-2015-STG-677467) and Science Foundation Ireland (SFI-16/ERCS/3787)

Brain Imaging Genetics (BIG): This work makes use of the BIG database, first established in Nijmegen, The Netherlands, in 2007. This resource is now part of Cognomics (www.cognomics.nl), a joint initiative by researchers from the Donders Centre for Cognitive Neuroimaging, the Human Genetics and Cognitive Neuroscience departments of the Radboud University Medical Centre, and the Max Planck Institute for Psycholinguistics in Nijmegen. The Cognomics Initiative has received support from the participating departments and centres and from external grants, that is, the Biobanking and Biomolecular Resources Research Infrastructure (Netherlands) (BBMRI-NL), the Hersenstichting Nederland and the Netherlands Organization for Scientific Research (NWO). The research leading to these results also receives funding from the NWO Gravitation Grant 024.001.006 'Language in Interaction', the European Community's Seventh Framework Programme (FP7/2007-2013) under grant agreement nos. 602450 (IMAGEMEND), 278948 (TACTICS) and 602805 (Aggressotype), as well as from the European Community's Horizon 2020 programme under grant agreement no. 643051 (MiND) and from ERC-2010-AdG 268800-NEUROSCHEMA. In addition, the work was supported by a grant for the ENIGMA Consortium (grant number U54 EB020403) from the BD2K Initiative of a cross-NIH partnership.

Disclosures

Dr. Andreassen has received speakers honorarium from Lundbeck, Janssen and Sunovion, and is a consultant to coretechs.ai. Dr. Reis Marques reports personal fees from Pfizer, Lundbeck, Astellas, Janssen and Angelini outside the submitted work. He is an employee and shareholder of Pasithea Therapeutics. Dr. Ching has received partial research support from Biogen, Inc. (Boston, USA) for work unrelated to the topic of this manuscript (PI Paul

Thompson). Dr. Thompson has received partial research support from Biogen, Inc. (Boston, USA) for work unrelated to the topic of this manuscript. Dr. van den Bree reports grants from Takeda Pharmaceuticals, outside the submitted work. Dr. Grabe has received travel grants and speakers honoraria from Fresenius Medical Care, Neuraxpharm, Servier and Janssen Cilag as well as research funding from Fresenius Medical Care. All other authors declare no competing financial interests.

References

1. Calle Sánchez, X. *et al.* Comparing Copy Number Variations in a Danish Case Cohort of Individuals With Psychiatric Disorders. *JAMA Psychiatry* **79**, 59–69 (2022).
2. Stefansson, H. *et al.* Large recurrent microdeletions associated with schizophrenia. *Nature* **455**, 232–236 (2008).
3. Marshall, C. R. *et al.* Contribution of copy number variants to schizophrenia from a genome-wide study of 41,321 subjects. *Nat. Genet.* **49**, 27–35 (2017).
4. Singh, T. *et al.* Rare coding variants in ten genes confer substantial risk for schizophrenia. *Nature* **604**, 509–516 (2022).
5. Mollon, J., Almasy, L., Jacquemont, S. & Glahn, D. C. The contribution of copy number variants to psychiatric symptoms and cognitive ability. *Mol. Psychiatry* 1–14 (2023) doi:10.1038/s41380-023-01978-4.
6. Modenato, C. *et al.* Lessons Learned From Neuroimaging Studies of Copy Number Variants: A Systematic Review. *Biol. Psychiatry* **90**, 596–610 (2021).
7. Sønderby, I. E. *et al.* Effects of copy number variations on brain structure and risk for psychiatric illness: Large-scale studies from the ENIGMA working groups on CNVs. *Hum. Brain Mapp.* **43**, 300–328 (2022).
8. Moreau, C. A., Ching, C. R., Kumar, K., Jacquemont, S. & Bearden, C. E. Structural and functional brain alterations revealed by neuroimaging in CNV carriers. *Curr. Opin. Genet. Dev.* **68**, 88–98 (2021).
9. Chapman, G. *et al.* Using induced pluripotent stem cells to investigate human neuronal phenotypes in 1q21.1 deletion and duplication syndrome. *Mol. Psychiatry* **27**, 819–830 (2022).
10. Urresti, J. *et al.* Cortical organoids model early brain development disrupted by 16p11.2 copy number variants in autism. *Mol. Psychiatry* **26**, 7560–7580 (2021).

11. Khan, T. A. *et al.* Neuronal defects in a human cellular model of 22q11.2 deletion syndrome. *Nat. Med.* **26**, 1888–1898 (2020).

12. Sundberg, M. *et al.* 16p11.2 deletion is associated with hyperactivation of human iPSC-derived dopaminergic neuron networks and is rescued by RHOA inhibition in vitro. *Nat. Commun.* **12**, 2897 (2021).

13. Smajlagić, D. *et al.* Population prevalence and inheritance pattern of recurrent CNVs associated with neurodevelopmental disorders in 12,252 newborns and their parents. *Eur. J. Hum. Genet.* **29**, 205–215 (2021).

14. Kendall, K. M. *et al.* Cognitive Performance Among Carriers of Pathogenic Copy Number Variants: Analysis of 152,000 UK Biobank Subjects. *Biol. Psychiatry* **82**, 103–110 (2017).

15. Sønderby, I. E. *et al.* 1q21.1 distal copy number variants are associated with cerebral and cognitive alterations in humans. *Transl. Psychiatry* **11**, 1–16 (2021).

16. Writing Committee for the ENIGMA-CNV Working Group *et al.* Association of Copy Number Variation of the 15q11.2 BP1-BP2 Region With Cortical and Subcortical Morphology and Cognition. *JAMA Psychiatry* **77**, 420–430 (2020).

17. Anderson, A. E. *et al.* Intra-individual variability in neuropsychological performance predicts cognitive decline and death in HIV. *Neuropsychology* **32**, 966–972 (2018).

18. Dykiert, D., Der, G., Starr, J. M. & Deary, I. J. Sex differences in reaction time mean and intraindividual variability across the life span. *Dev. Psychol.* **48**, 1262–1276 (2012).

19. Hilborn, J. V., Strauss, E., Hultsch, D. F. & Hunter, M. A. Intraindividual variability across cognitive domains: Investigation of dispersion levels and performance profiles in older adults. *J. Clin. Exp. Neuropsychol.* **31**, 412–424 (2009).

20. MacDonald, S. W. S., Nyberg, L. & Bäckman, L. Intra-individual variability in

behavior: links to brain structure, neurotransmission and neuronal activity. *Trends Neurosci.* **29**, 474–480 (2006).

21. Roalf, D. R. *et al.* Within-Individual Variability: An Index for Subtle Change in Neurocognition in Mild Cognitive Impairment. *J. Alzheimers Dis. JAD* **54**, 325–335 (2016).

22. Tamnes, C. K., Fjell, A. M., Westlye, L. T., Østby, Y. & Walhovd, K. B. Becoming Consistent: Developmental Reductions in Intraindividual Variability in Reaction Time Are Related to White Matter Integrity. *J. Neurosci.* **32**, 972–982 (2012).

23. Keller, A. S. *et al.* Hierarchical functional system development supports executive function. *Trends Cogn. Sci.* **27**, 160–174 (2023).

24. Sydnor, V. J. *et al.* Neurodevelopment of the association cortices: Patterns, mechanisms, and implications for psychopathology. *Neuron* **109**, 2820–2846 (2021).

25. Yeo, B. T. T. *et al.* Functional Specialization and Flexibility in Human Association Cortex. *Cereb. Cortex* **25**, 3654–3672 (2015).

26. Ho, D., Imai, K., King, G. & Stuart, E. A. MatchIt: Nonparametric Preprocessing for Parametric Causal Inference. *J. Stat. Softw.* **42**, 1–28 (2011).

27. Alfaro-Almagro, F. *et al.* Image processing and Quality Control for the first 10,000 brain imaging datasets from UK Biobank. *NeuroImage* **166**, 400–424 (2018).

28. Monereo-Sánchez, J. *et al.* Quality control strategies for brain MRI segmentation and parcellation: Practical approaches and recommendations - insights from the Maastricht study. *NeuroImage* **237**, 118174 (2021).

29. Radua, J. *et al.* Increased power by harmonizing structural MRI site differences with the ComBat batch adjustment method in ENIGMA. *NeuroImage* **218**, 116956 (2020).

30. Crawford, K. *et al.* Medical consequences of pathogenic CNVs in adults: analysis of the UK Biobank. *J. Med. Genet.* **56**, 131–138 (2019).

31. Kochunov, P. *et al.* White Matter in Schizophrenia Treatment Resistance. *Am. J. Psychiatry* **176**, 829–838 (2019).

32. Larivière, S. *et al.* The ENIGMA Toolbox: multiscale neural contextualization of multisite neuroimaging datasets. *Nat. Methods* **18**, 698–700 (2021).

33. Benjamini, Y. & Hochberg, Y. Controlling the False Discovery Rate: A Practical and Powerful Approach to Multiple Testing. *J. R. Stat. Soc. Ser. B Methodol.* **57**, 289–300 (1995).

34. Stefansson, H. *et al.* CNVs conferring risk of autism or schizophrenia affect cognition in controls. *Nature* **505**, 361–366 (2014).

35. Cox, D. M. & Butler, M. G. The 15q11.2 BP1–BP2 Microdeletion Syndrome: A Review. *Int. J. Mol. Sci.* **16**, 4068–4082 (2015).

36. van Rooij, D. *et al.* Cortical and Subcortical Brain Morphometry Differences Between Patients With Autism Spectrum Disorder and Healthy Individuals Across the Lifespan: Results From the ENIGMA ASD Working Group. *Am. J. Psychiatry* **175**, 359–369 (2018).

37. van Erp, T. G. M. *et al.* Cortical Brain Abnormalities in 4474 Individuals With Schizophrenia and 5098 Control Subjects via the Enhancing Neuro Imaging Genetics Through Meta Analysis (ENIGMA) Consortium. *Biol. Psychiatry* **84**, 644–654 (2018).

38. Fiddes, I. T. *et al.* Human-Specific NOTCH2NL Genes Affect Notch Signaling and Cortical Neurogenesis. *Cell* **173**, 1356-1369.e22 (2018).

39. Suzuki, I. K. *et al.* Human-Specific NOTCH2NL Genes Expand Cortical Neurogenesis through Delta/Notch Regulation. *Cell* **173**, 1370-1384.e16 (2018).

40. Hansen, D. V., Lui, J. H., Parker, P. R. L. & Kriegstein, A. R. Neurogenic radial glia in the outer subventricular zone of human neocortex. *Nature* **464**, 554–561 (2010).

41. Florio, M. *et al.* Evolution and cell-type specificity of human-specific genes

preferentially expressed in progenitors of fetal neocortex. *eLife* **7**, e32332 (2018).

42. Chai, J.-H. *et al.* Identification of Four Highly Conserved Genes between Breakpoint Hotspots BP1 and BP2 of the Prader-Willi/Angelman Syndromes Deletion Region That Have Undergone Evolutionary Transposition Mediated by Flanking Duplicons. *Am. J. Hum. Genet.* **73**, 898–925 (2003).

43. Tam, G. W. C. *et al.* Confirmed rare copy number variants implicate novel genes in schizophrenia. *Biochem. Soc. Trans.* **38**, 445–451 (2010).

44. Nebel, R. A. *et al.* Reduced CYFIP1 in Human Neural Progenitors Results in Dysregulation of Schizophrenia and Epilepsy Gene Networks. *PLOS ONE* **11**, e0148039 (2016).

45. Wang, J. *et al.* Common Regulatory Variants of CYFIP1 Contribute to Susceptibility for Autism Spectrum Disorder (ASD) and Classical Autism. *Ann. Hum. Genet.* **79**, 329–340 (2015).

46. Toma, C. *et al.* Exome sequencing in multiplex autism families suggests a major role for heterozygous truncating mutations. *Mol. Psychiatry* **19**, 784–790 (2014).

47. Zwaag, B. van der *et al.* A co-segregating microduplication of chromosome 15q11.2 pinpoints two risk genes for autism spectrum disorder. *Am. J. Med. Genet. B Neuropsychiatr. Genet.* **153B**, 960–966 (2010).

48. Woo, Y. J. *et al.* A Common CYFIP1 Variant at the 15q11.2 Disease Locus Is Associated with Structural Variation at the Language-Related Left Supramarginal Gyrus. *PLOS ONE* **11**, e0158036 (2016).

49. Silva, A. I. *et al.* Cyfip1 haploinsufficient rats show white matter changes, myelin thinning, abnormal oligodendrocytes and behavioural inflexibility. *Nat. Commun.* **10**, 3455 (2019).

50. Oguro-Ando, A. *et al.* Increased CYFIP1 dosage alters cellular and dendritic

morphology and dysregulates mTOR. *Mol. Psychiatry* **20**, 1069–1078 (2015).

51. De Rubeis, S. *et al.* CYFIP1 Coordinates mRNA Translation and Cytoskeleton Remodeling to Ensure Proper Dendritic Spine Formation. *Neuron* **79**, 1169–1182 (2013).

52. Yoon, K.-J. *et al.* Modeling a Genetic Risk for Schizophrenia in iPSCs and Mice Reveals Neural Stem Cell Deficits Associated with Adherens Junctions and Polarity. *Cell Stem Cell* **15**, 79–91 (2014).

53. Natu, V. S. *et al.* Apparent thinning of human visual cortex during childhood is associated with myelination. *Proc. Natl. Acad. Sci.* 201904931 (2019) doi:10.1073/pnas.1904931116.

54. Domínguez-Iturza, N. *et al.* The autism- and schizophrenia-associated protein CYFIP1 regulates bilateral brain connectivity and behaviour. *Nat. Commun.* **10**, 3454 (2019).

55. Jensen, M. & Girirajan, S. An interaction-based model for neuropsychiatric features of copy-number variants. *PLOS Genet.* **15**, e1007879 (2019).

56. Fry, A. *et al.* Comparison of Sociodemographic and Health-Related Characteristics of UK Biobank Participants With Those of the General Population. *Am. J. Epidemiol.* **186**, 1026–1034 (2017).

Figure 1. Cortical surface area comparison between 1q21.1 distal deletion carriers and non-carriers. A) Top panel shows z-scores - group differences in regional cortical surface area. Bottom panel shows RID-scores - group differences in regional cortical surface area that are scaled to the individual's own global index. Non-carriers are represented by gray lines, and 1q21.1 distal deletion carriers are represented by black lines. Blue dots indicate significant differences. The insular cortex is included under frontal cortex for visualization purposes. B) Top panel displays the significant differences in Z-scores, and the bottom panel shows the significant differences in RID-scores. Blue-red diverging maps represent the effect size. C) Spatial distribution of all the mean differences in RID scores. Please note that all values are shown regardless of significance. Yellow-purple diverging maps represent the direction of the mean differences. Increased yellow intensity represents values that are less deviant than the overall global mean difference in cortical surface area, and increased purple intensity represents values that are more deviant than the overall global mean difference in cortical surface area. Z- and RID-scores are based on raw values adjusted for age, age^2, sex, and intracranial volume on site harmonized data.

Figure 2. Cortical thickness comparison between 1q21.1 distal deletion carriers and non-carriers. A) Top panel shows z-scores - group differences in regional cortical thickness. Bottom panel shows RID-scores - group differences in regional cortical thickness that are scaled to the individual's own global index. Non-carriers are represented by gray lines, and 1q21.1 distal deletion carriers are represented by black lines. Blue dots indicate significant differences. The insular cortex is included under frontal cortex for visualization purposes. B) Top panel displays the significant differences in Z-scores, and the bottom panel shows the significant differences in RID-scores. Blue-red diverging maps represent the effect size. C) Spatial distribution of all the mean differences in RID scores. Please note that all values are

shown regardless of significance. Yellow-purple diverging maps represent the direction of the mean differences. Increased yellow intensity represents values that are less deviant than the overall global mean difference in cortical thickness, and increased purple intensity represents values that are more deviant than the overall global mean difference in cortical thickness. Z- and RID-scores are based on raw values adjusted for age, age^2, sex, and intracranial volume on site harmonized data.

Figure 3. Cortical surface area comparison between 15q11.2 BP1-BP2 deletion carriers and non-carriers. A) Top panel shows z-scores - group differences in regional cortical surface area. Bottom panel shows RID-scores - group differences in regional cortical surface area that are scaled to the individual's own global index. Non-carriers are represented by gray lines, and 15q11.2 BP1-BP2 deletion carriers are represented by black lines. Blue dots indicate significant differences. The insular cortex is included under frontal cortex for visualization purposes. B) Top panel displays the significant differences in Z-scores, and the bottom panel shows the significant differences in RID-scores. Blue-red diverging maps represent the effect size. C) Spatial distribution of all the mean differences in RID scores. Please note that all values are shown regardless of significance. Yellow-purple diverging maps represent the direction of the mean differences. Increased yellow intensity represents values that are less deviant than the overall global mean difference in cortical surface area, and increased purple intensity represents values that are more deviant than the overall global mean difference in cortical surface area. Z- and RID-scores are based on raw values adjusted for age, age^2, sex, and intracranial volume on site harmonized data.

Figure 4. Cortical thickness comparison between 15q11.2 BP1-BP2 deletion carriers and non-carriers. A) Top panel shows z-scores - group differences in regional cortical thickness.

Bottom panel shows RID-scores - group differences in regional cortical thickness that are scaled to the individual's own global index. Non-carriers are represented by gray lines, and 15q11.2 BP1-BP2 deletion carriers are represented by black lines. Blue dots indicate significant differences. The insular cortex is included under frontal cortex for visualization purposes. B) Top panel displays the significant differences in Z-scores, and the bottom panel shows the significant differences in RID-scores. Blue-red diverging maps represent the effect size. C) Spatial distribution of all the mean differences in RID scores. Please note that all values are shown regardless of significance. Yellow-purple diverging maps represent the direction of the mean differences. Increased yellow intensity represents values that are less deviant than the overall global mean difference in cortical thickness, and increased purple intensity represents values that are more deviant than the overall global mean difference in cortical thickness. Z- and RID-scores are based on raw values adjusted for age, age^2, sex, and intracranial volume on site harmonized data.

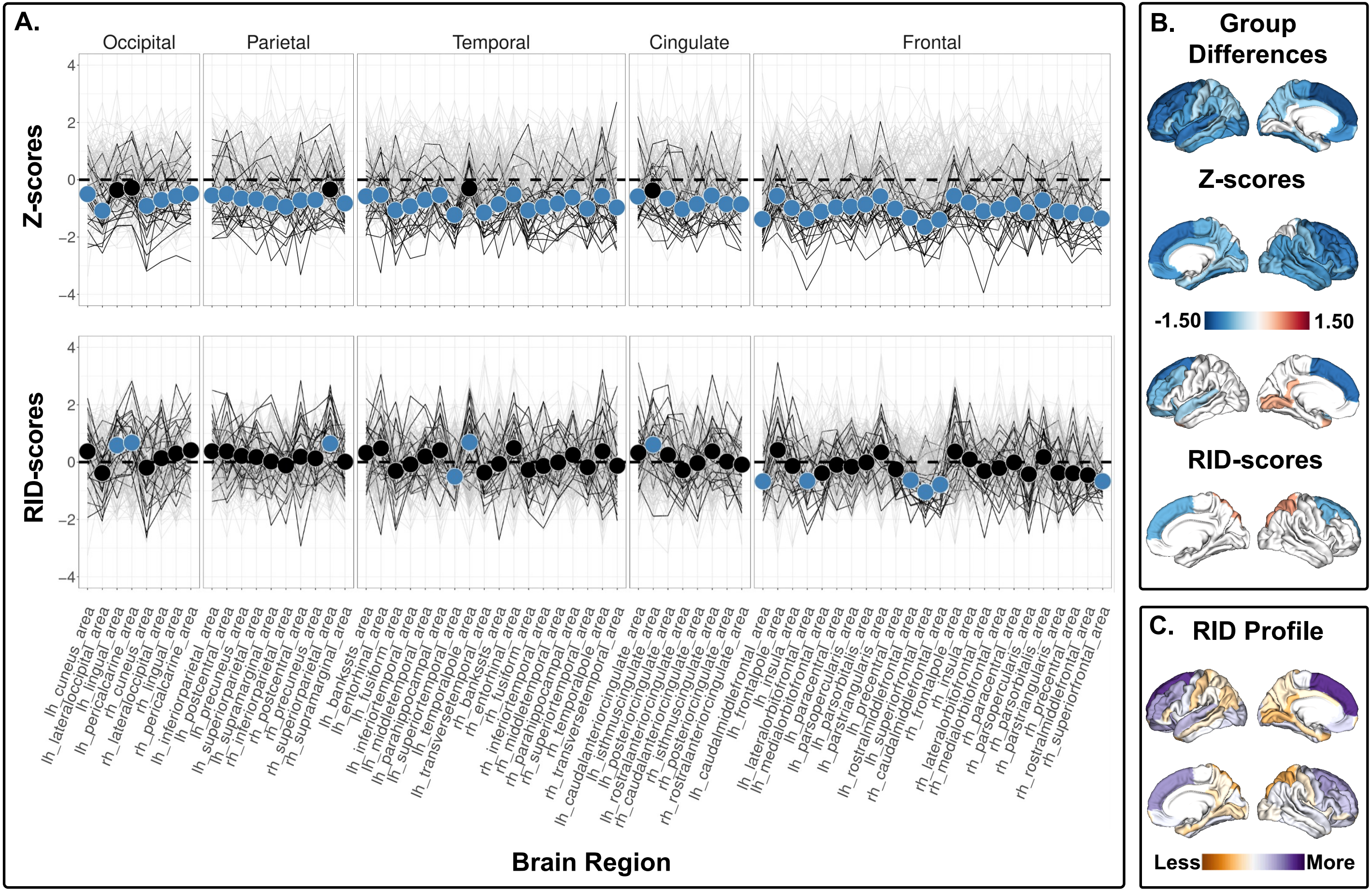

A.
Occipital
Parietal
Temporal
Cingulate
Frontal
Z-scores
RID-scores
4
2
0
−2
−4
lh_cuneus_area
lh_lateraloccipital_area
lh_lingual_area
lh_pericalcarine_area
rh_cuneus_area
rh_lateraloccipital_area
rh_lingual_area
rh_pericalcarine_area
lh_inferiorparietal_area
lh_postcentral_area
lh_precuneus_area
lh_superiorparietal_area
lh_supramarginal_area
rh_inferiorparietal_area
rh_postcentral_area
rh_precuneus_area
rh_superiorparietal_area
rh_supramarginal_area
lh_bankssts_area
lh_entorhinal_area
lh_fusiform_area
lh_inferiortemporal_area
lh_middletemporal_area
lh_parahippocampal_area
lh_superiortemporal_area
lh_temporalpole_area
lh_transversetemporal_area
rh_bankssts_area
rh_entorhinal_area
rh_fusiform_area
rh_inferiortemporal_area
rh_middletemporal_area
rh_parahippocampal_area
rh_superiortemporal_area
rh_temporalpole_area
rh_transversetemporal_area
lh_caudalanteriorcingulate_area
lh_isthmuscingulate_area
lh_posteriorcingulate_area
lh_rostralanteriorcingulate_area
rh_caudalanteriorcingulate_area
rh_isthmuscingulate_area
rh_posteriorcingulate_area
rh_rostralanteriorcingulate_area
lh_caudalmiddlefrontal_area
lh_frontalpole_area
lh_insula_area
lh_lateralorbitofrontal_area
lh_medialorbitofrontal_area
lh_paracentral_area
lh_parsopercularis_area
lh_parsorbitalis_area
lh_parstriangularis_area
lh_precentral_area
lh_rostralmiddlefrontal_area
lh_superiorfrontal_area
rh_caudalmiddlefrontal_area
rh_frontalpole_area
rh_insula_area
rh_lateralorbitofrontal_area
rh_medialorbitofrontal_area
rh_paracentral_area
rh_parsopercularis_area
rh_parsorbitalis_area
rh_parstriangularis_area
rh_precentral_area
rh_rostralmiddlefrontal_area
rh_superiorfrontal_area
Brain Region
B.
Group Differences
Z-scores
-1.50
1.50
RID-scores
C.
RID Profile
Less
More

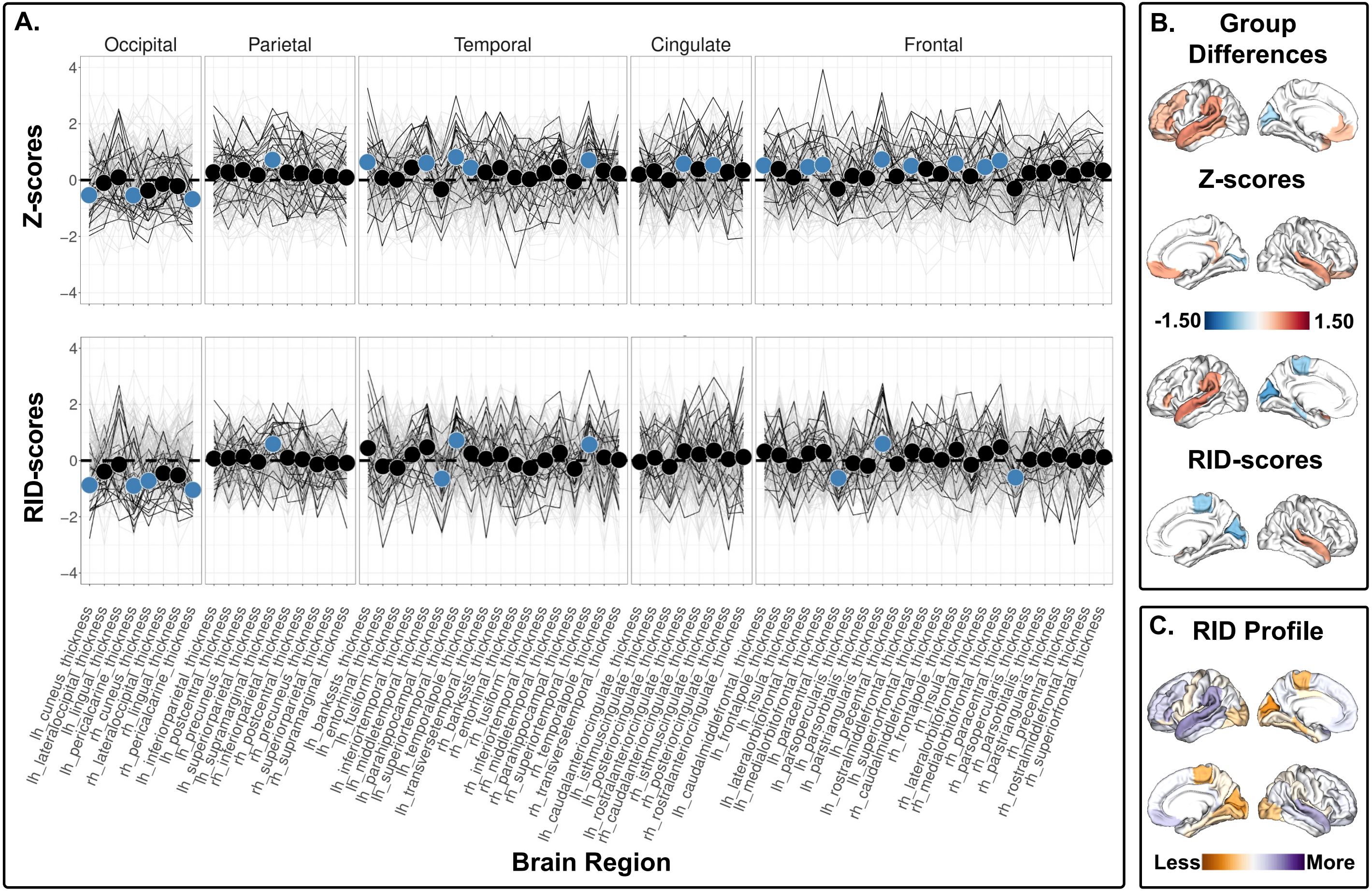
A.
Occipital
Parietal
Temporal
Cingulate
Frontal
Z-scores
RID-scores
4
2
0
−2
−4
lh_cuneus_thickness
lh_lateraloccipital_thickness
lh_lingual_thickness
lh_pericalcarine_thickness
rh_cuneus_thickness
rh_lateraloccipital_thickness
rh_lingual_thickness
rh_pericalcarine_thickness
lh_inferiorparietal_thickness
lh_postcentral_thickness
lh_precuneus_thickness
lh_superiorparietal_thickness
lh_supramarginal_thickness
rh_inferiorparietal_thickness
rh_postcentral_thickness
rh_precuneus_thickness
rh_superiorparietal_thickness
rh_supramarginal_thickness
lh_bankssts_thickness
lh_entorhinal_thickness
lh_fusiform_thickness
lh_inferiortemporal_thickness
lh_middletemporal_thickness
lh_parahippocampal_thickness
lh_superiortemporal_thickness
lh_temporalpole_thickness
lh_transversetemporal_thickness
rh_bankssts_thickness
rh_entorhinal_thickness
rh_fusiform_thickness
rh_inferiortemporal_thickness
rh_middletemporal_thickness
rh_parahippocampal_thickness
rh_superiortemporal_thickness
rh_temporalpole_thickness
rh_transversetemporal_thickness
lh_caudalanteriorcingulate_thickness
lh_isthmuscingulate_thickness
lh_posteriorcingulate_thickness
lh_rostralanteriorcingulate_thickness
rh_caudalanteriorcingulate_thickness
rh_isthmuscingulate_thickness
rh_posteriorcingulate_thickness
rh_rostralanteriorcingulate_thickness
lh_caudalmiddlefrontal_thickness
lh_frontalpole_thickness
lh_insula_thickness
lh_lateralorbitofrontal_thickness
lh_medialorbitofrontal_thickness
lh_paracentral_thickness
lh_parsopercularis_thickness
lh_parsorbitalis_thickness
lh_parstriangularis_thickness
lh_precentral_thickness
lh_rostralmiddlefrontal_thickness
lh_superiorfrontal_thickness
rh_caudalmiddlefrontal_thickness
rh_frontalpole_thickness
rh_insula_thickness
rh_lateralorbitofrontal_thickness
rh_medialorbitofrontal_thickness
rh_paracentral_thickness
rh_parsopercularis_thickness
rh_parsorbitalis_thickness
rh_parstriangularis_thickness
rh_precentral_thickness
rh_rostralmiddlefrontal_thickness
rh_superiorfrontal_thickness
Brain Region
B. Group Differences
Z-scores
-1.50
1.50
RID-scores
C. RID Profile
Less
More

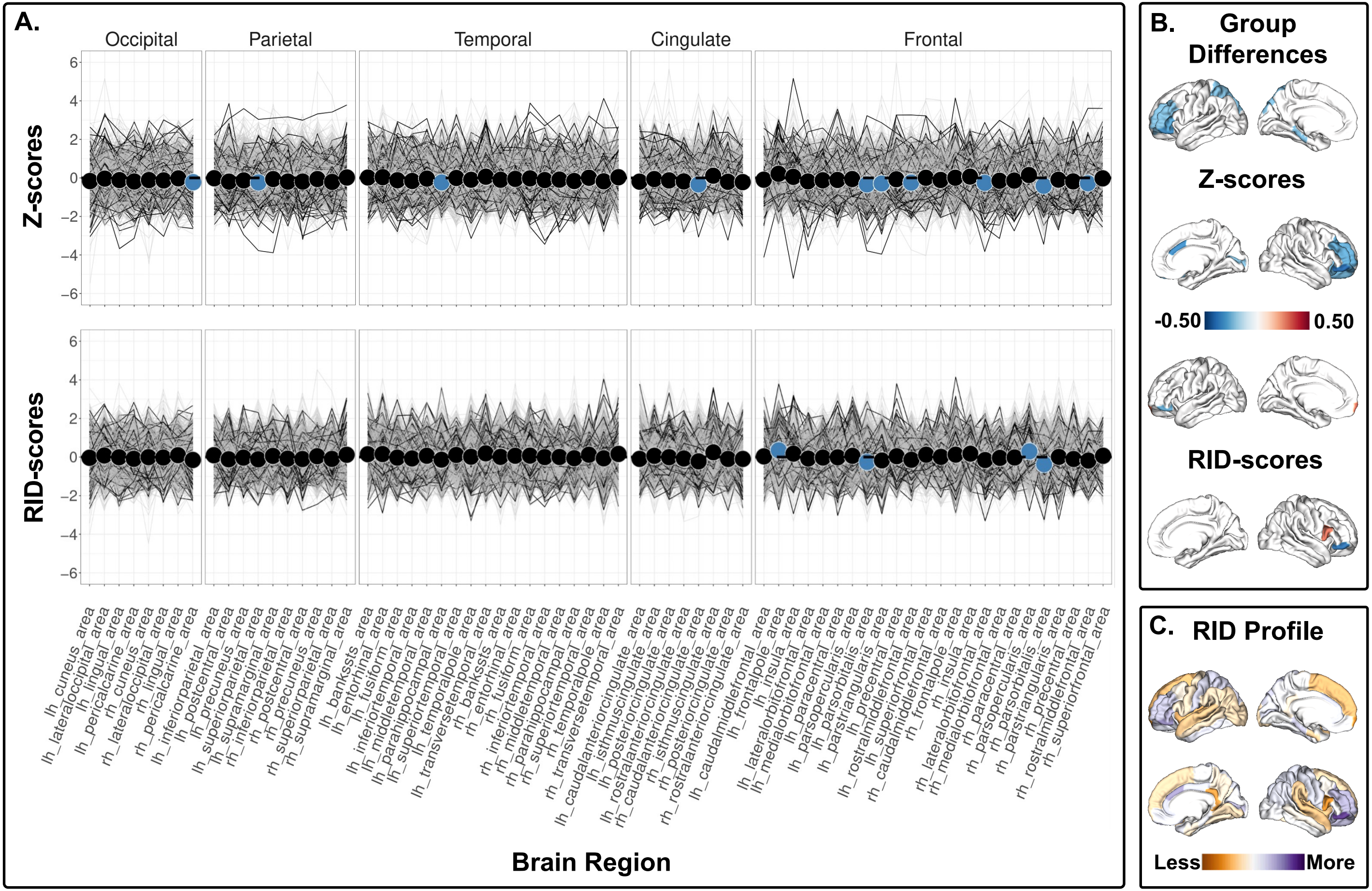
A.
Occipital
Parietal
Temporal
Cingulate
Frontal
Z-scores
RID-scores
Brain Region
lh_cuneus_area
lh_lateraloccipital_area
lh_lingual_area
lh_pericalcarine_area
rh_cuneus_area
rh_lateraloccipital_area
rh_lingual_area
rh_pericalcarine_area
lh_inferiorparietal_area
lh_postcentral_area
lh_precuneus_area
lh_superiorparietal_area
lh_supramarginal_area
rh_inferiorparietal_area
rh_postcentral_area
rh_precuneus_area
rh_superiorparietal_area
rh_supramarginal_area
lh_bankssts_area
lh_entorhinal_area
lh_fusiform_area
lh_inferiortemporal_area
lh_middletemporal_area
lh_parahippocampal_area
lh_superiortemporal_area
lh_temporalpole_area
lh_transversetemporal_area
rh_bankssts_area
rh_entorhinal_area
rh_fusiform_area
rh_inferiortemporal_area
rh_middletemporal_area
rh_parahippocampal_area
rh_superiortemporal_area
rh_temporalpole_area
rh_transversetemporal_area
lh_caudalanteriorcingulate_area
lh_isthmuscingulate_area
lh_posteriorcingulate_area
lh_rostralanteriorcingulate_area
rh_caudalanteriorcingulate_area
rh_isthmuscingulate_area
rh_posteriorcingulate_area
rh_rostralanteriorcingulate_area
lh_caudalmiddlefrontal_area
lh_frontalpole_area
lh_insula_area
lh_lateralorbitofrontal_area
lh_medialorbitofrontal_area
lh_paracentral_area
lh_parsopercularis_area
lh_parsorbitalis_area
lh_parstriangularis_area
lh_precentral_area
lh_rostralmiddlefrontal_area
lh_superiorfrontal_area
rh_caudalmiddlefrontal_area
rh_frontalpole_area
rh_insula_area
rh_lateralorbitofrontal_area
rh_medialorbitofrontal_area
rh_paracentral_area
rh_parsopercularis_area
rh_parsorbitalis_area
rh_parstriangularis_area
rh_precentral_area
rh_rostralmiddlefrontal_area
rh_superiorfrontal_area
B. Group Differences
Z-scores
-0.50
0.50
RID-scores
C. RID Profile
Less
More

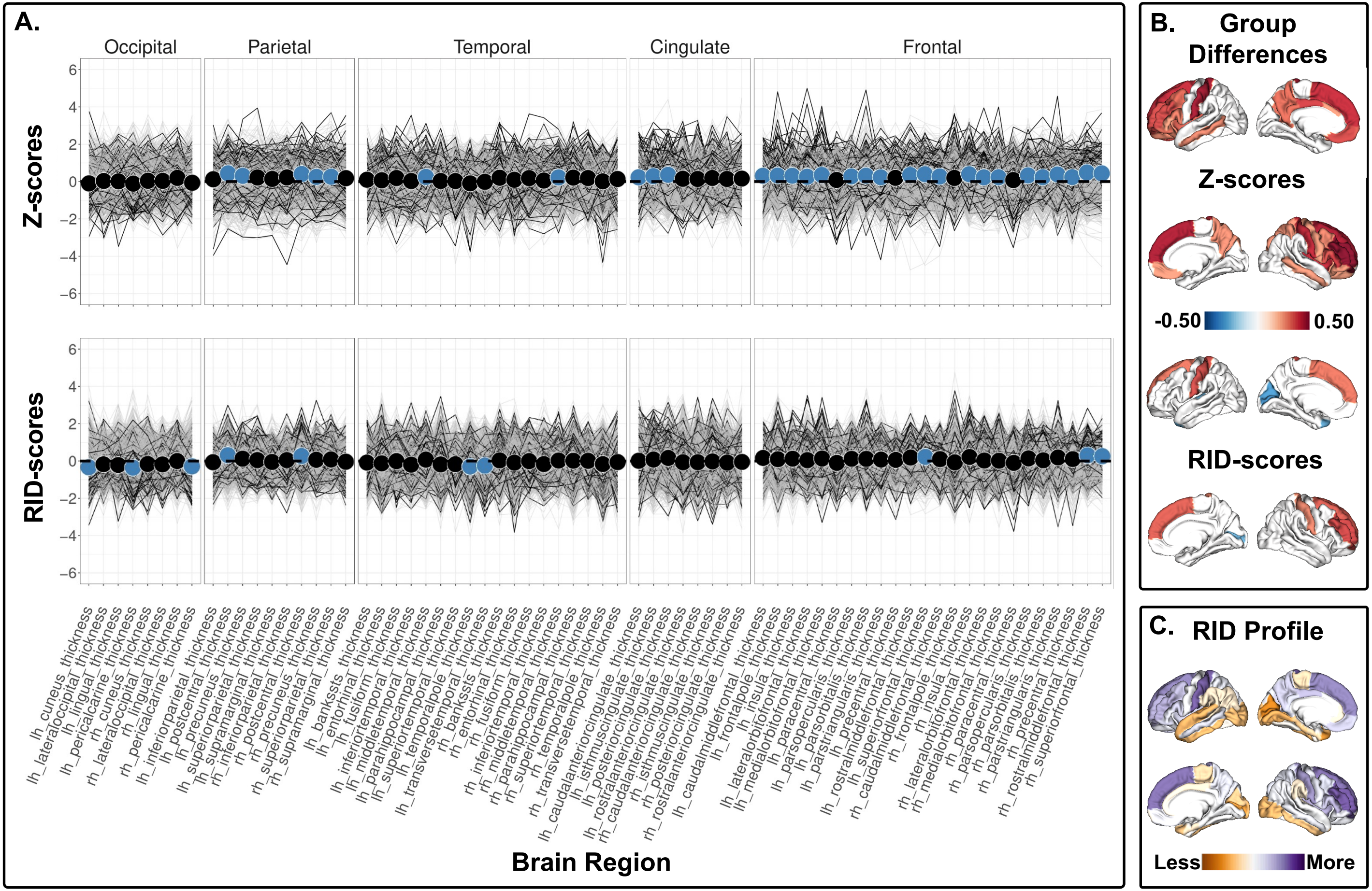
A.
Occipital
Parietal
Temporal
Cingulate
Frontal
Z-scores
RID-scores
6
4
2
0
−2
−4
−6
lh_cuneus_thickness
lh_lateraloccipital_thickness
lh_lingual_thickness
lh_pericalcarine_thickness
rh_cuneus_thickness
rh_lateraloccipital_thickness
rh_lingual_thickness
rh_pericalcarine_thickness
lh_inferiorparietal_thickness
lh_postcentral_thickness
lh_precuneus_thickness
lh_superiorparietal_thickness
lh_supramarginal_thickness
rh_inferiorparietal_thickness
rh_postcentral_thickness
rh_precuneus_thickness
rh_superiorparietal_thickness
rh_supramarginal_thickness
lh_bankssts_thickness
lh_entorhinal_thickness
lh_fusiform_thickness
lh_inferiortemporal_thickness
lh_middletemporal_thickness
lh_parahippocampal_thickness
lh_superiortemporal_thickness
lh_temporalpole_thickness
lh_transversetemporal_thickness
rh_bankssts_thickness
rh_entorhinal_thickness
rh_fusiform_thickness
rh_inferiortemporal_thickness
rh_middletemporal_thickness
rh_parahippocampal_thickness
rh_superiortemporal_thickness
rh_temporalpole_thickness
rh_transversetemporal_thickness
lh_caudalanteriorcingulate_thickness
lh_isthmuscingulate_thickness
lh_posteriorcingulate_thickness
lh_rostralanteriorcingulate_thickness
rh_caudalanteriorcingulate_thickness
rh_isthmuscingulate_thickness
rh_posteriorcingulate_thickness
rh_rostralanteriorcingulate_thickness
lh_caudalmiddlefrontal_thickness
lh_frontalpole_thickness
lh_insula_thickness
lh_lateralorbitofrontal_thickness
lh_medialorbitofrontal_thickness
lh_paracentral_thickness
lh_parsopercularis_thickness
lh_parsorbitalis_thickness
lh_parstriangularis_thickness
lh_precentral_thickness
lh_rostralmiddlefrontal_thickness
lh_superiorfrontal_thickness
rh_caudalmiddlefrontal_thickness
rh_frontalpole_thickness
rh_insula_thickness
rh_lateralorbitofrontal_thickness
rh_medialorbitofrontal_thickness
rh_paracentral_thickness
rh_parsopercularis_thickness
rh_parsorbitalis_thickness
rh_parstriangularis_thickness
rh_precentral_thickness
rh_rostralmiddlefrontal_thickness
rh_superiorfrontal_thickness
Brain Region
B. Group Differences
Z-scores
-0.50
0.50
RID-scores
C. RID Profile
Less
More